

# Interpretation of ferroelectric domain images recorded with piezoresponse force microscopy

T. Jungk,\* A. Hoffmann, and E. Soergel

*Institute of Physics, University of Bonn,*

*Wegelerstraße 8, 53115 Bonn, Germany*

(Dated: January 23, 2019)

## Abstract

The interpretation of ferroelectric domain images obtained with piezoresponse force microscopy (PFM) is discussed. The influences of an inherent experimental background on the domain contrast in PFM images (enhancement, nulling, inversion) as well as on the shape and the location of the domain boundaries are described. We present experimental results to evidence our analysis of the influence of the background on the domain contrast in PFM images.

PACS numbers: 77.80.Dj, 68.37.Ps, 77.84.-s

---

\*Electronic address: jungk@physik.uni-bonn.de

## Introduction

Ferroelectric domain patterns are the basis of a multitude of applications such as quasi-phase-matched frequency converters [1], electro-optic scanners [2], nonlinear photonic crystals [3], and ultra-high density data storage devices [4]. For the visualization of ferroelectric domains several techniques have been developed [5], however, selective etching [6] and piezoresponse force microscopy [7] are by far the most utilized. Selective etching is popular because it gives a simple and rapid estimate of the domain structure over large areas, however, it is destructive. Piezoresponse force microscopy, even though the image size is restricted to about  $100 \times 100 \mu\text{m}^2$ , is widely used because of its high lateral resolution and non-destructive imaging capability. Furthermore, the possibility to modify the domain structure with the help of its sharp tip [4] makes the piezoresponse force microscope (PFM) a versatile tool for the investigation of ferroelectric domains and domain boundaries. Although domain structures are easily imaged with this method, the interpretation of the obtained images, however, is still challenging because of the complexity of the detection mechanism.

Piezoresponse force microscopy is based on the deformation of the sample due to the converse piezoelectric effect. The PFM is a scanning force microscope (SFM) operated in contact mode with an additional alternating voltage applied to the tip. In piezoelectric samples this voltage causes thickness changes and therefore vibrations of the surface which lead to oscillations of the cantilever that can be read out with a lock-in amplifier. The different orientations of the polar axis of adjacent domains lead to a domain contrast in PFM measurements, i. e., the domains are for example displayed as bright and dark areas in PFM images. However, in a previous paper [8], we have shown that the PFM measurements are usually governed by a background which is inherent to the experimental setup. This background leads to a domain contrast whose amplitude and phase depends on the frequency of the alternating voltage applied to the tip [9, 10, 11, 12, 13, 14, 15, 16, 17]: the measured oscillation amplitudes of the cantilever are usually larger than the theoretically expected values and the expected phase difference of  $180^\circ$  between adjacent domains is not always obtained. Furthermore, this background can influence shape and location of the domain boundaries.

The aim of this contribution is to point out possible causes for the misinterpretation of PFM images and to propose experimental settings to achieve unambiguous data. A simple

model allows a quantitative estimate of the contribution of the background to the domain contrast in PFM images. The considerations presented in this paper might provide a deeper insight into PFM measurements and should be taken into account when drawing conclusions from images of ferroelectric domains and domain boundaries obtained with piezoresponse force microscopy.

### Experimental conditions

To utilize a SFM for piezoresponse force microscopy requires mainly two instrumental features: (i) an electrical connection to the tip and (ii) a direct access to the signals recording the movement of the cantilever. We will restrict ourselves here only to the vertical cantilever movement, i. e., its bending normal to the surface. Furthermore, an external lock-in amplifier is necessary for sensitive readout of the cantilever movement.

In the following the crucial parts of the experimental setup are described in order to clearly define the parameters and denotations later used in the text. In addition, our experimental standard settings for PFM operation are given:

- Tip of the SFM: For PFM operation the tip must be conductive and electrically connected to allow the application of voltages. The resonance frequency of the cantilever is not crucial, it should however be far away from the frequency of the alternating voltage applied to the tip. Typically cantilevers with resonance frequencies  $f_0 \gg 100$  kHz are utilized. The alternating voltage is generally chosen to have a frequency between 10 kHz and 100 kHz with an amplitude  $U \leq 20$  V<sub>pp</sub>. The time constant of the feedback-loop of the SFM must be chosen to be large compared to the period of modulation of the applied voltage to the tip to avoid a compensation of the signal.

We utilize Ti-Pt coated tips (MicroMasch) with resonance frequencies  $f_0 = 150 - 400$  kHz, spring constants  $k = 5 - 50$  N/m and apply an alternating voltage of  $f \approx 38$  kHz with an amplitude of 10 V<sub>pp</sub>.

- Sample: In large part PFM measurements are performed with crystals exhibiting only antiparallel domain structures. For investigation the samples are cut in such way, that the domain boundaries are perpendicular to the surface to be studied. We will restrict ourselves here only to such a configuration.

In the experiments presented here, we used a 0.5 mm thick,  $z$ -cut, periodically-poled LiNbO<sub>3</sub> crystal (PPLN) with a period length of 30  $\mu\text{m}$ .

- SFM: Generally all scanning force microscopes are suited for PFM operation as long as they allow application of voltages to the tip and separate readout of the cantilever movement.

We use a SMENA SFM (NT-MDT), modified to apply voltages to the tip and upgraded with an additional interface board for readout of the cantilever movement. Typical scanning velocity is about 1  $\mu\text{m/s}$ .

- Lock-in amplifier: Most PFM setups use dual-phase lock-in amplifiers which allow to choose between two output schemes: (i) in-phase output (also denoted as  $X$ -channel) and orthogonal output ( $Y$ -channel) or (ii) magnitude  $R = \sqrt{x^2 + y^2}$  and angle  $\theta = \arctan(Y/X)$ . These output signals of the lock-in amplifier will be named PFM-signals  $P$ . To specify the particular output channel, the adequate symbol ( $X, Y, R$  or  $\theta$ ) will be added as a subscript; to indicate on which domain face the signal is obtained  $\pm z$  will be added as a superscript. For example  $P_X^{+z}$  denotes the signal of the in-phase output of the lock-in amplifier on a positive domain face.

The experiments presented in this contribution are performed with a SRS 830 lock-in amplifier (Stanford Research Systems). Typical settings are 1 mV for the sensitivity and 1 ms for the time constant.

The aim of PFM measurements is to detect a deformation of the sample due to the converse piezoelectric effect. The response, i. e. the thickness change of the crystal, will be denoted as the piezoresponse signal  $\vec{d}$ . Depending on the orientation of the polar axis,  $\vec{d}$  is either in phase or of out of phase by 180° with respect to the alternating voltage applied to the tip. Unfortunately, PFM measurements are generally dominated by a system-inherent, frequency-dependent background [8]. The background signal, denoted as  $\vec{P}^b$  in the following, can be expressed as the average of the PFM-signals on a  $+z$  and a  $-z$  domain face:  $\vec{P}^b = \frac{1}{2}(\vec{P}^{+z} + \vec{P}^{-z})$ . Note that both, the piezoresponse and the background signal, are not directly accessible, but they must be calculated from the measured PFM-signals.

## Vectorial description of the PFM detection

For the correct interpretation of PFM measurements it is necessary to take into account the full data content of the PFM-signals, i. e. both, their magnitude and their phase with respect to the alternating voltage applied to the tip. We therefore describe the PFM-signals as vectors in the  $P_X$ ,  $P_Y$  plane. Figure 1(a) shows the vector diagram of PFM detection on a sample with  $+z$  and  $-z$  domain faces for one specific frequency [8]. The piezoresponse signals ( $-\vec{d}$  and  $\vec{d}$ ) have a phase of either  $0^\circ$  or  $180^\circ$  with respect to the alternating voltage applied to the tip and sit on top of the system-inherent background signal  $\vec{P}^b$ . Reading out the magnitude  $R$  of the lock-in amplifier leads to PFM-signals of  $P_R^{+z} = |\vec{P}^{+z}|$  on a  $+z$  domain face and  $P_R^{-z} = |\vec{P}^{-z}|$  on a  $-z$  domain face respectively. As it can be easily seen (Fig. 1(a)), the magnitude of these two PFM-signals is not equal and they are both larger than the expected value  $d = |\vec{d}|$  of the piezoresponse signal. Furthermore, their relative phase is by far not  $180^\circ$ , although,  $\vec{d}$  and  $-\vec{d}$  exhibit a  $180^\circ$  phase difference. These phenomena are due to the background signal  $\vec{P}^b$  which can reach amplitudes larger than the piezoresponse signal. Note that of course also  $\vec{P}^b$  can be separated into an in-phase  $P_X^b$  and an out-of-phase  $P_Y^b$  component.

To illustrate the importance of the system-inherent background signal  $\vec{P}^b$ , its dependence on the frequency of the alternating voltage applied to the tip is shown for one specific cantilever in Fig. 1(b). The frequency of the applied voltage of  $10 \text{ V}_{\text{pp}}$  is scanned from  $10 \text{ kHz}$  to  $100 \text{ kHz}$ . It is obvious that phase and amplitude of the background signal vary almost arbitrarily with frequency,  $\vec{P}^b$  being equally distributed on all four quadrants of the coordinate plane. The background signal depends strongly on the frequency: the big loop has a frequency span of  $3 \text{ kHz}$  only ( $39 \text{ kHz}$  -  $42 \text{ kHz}$ ; see also Fig. 1(d) from Ref. [8] which was obtained with the same cantilever). The amplitude of the background signal is generally  $\lesssim 100 \text{ pm}$  (except for the big loop), which is of the same order of magnitude as the piezoresponse signal  $d$  expected for the vibrations of the surface due to the converse piezoelectric effect for a  $z$ -cut  $\text{LiNbO}_3$  of  $76 \text{ pm}$  with  $10 \text{ V}_{\text{pp}}$  applied to the tip [18].

## Consequences of the background signal on PFM images

The existence of the background signal has serious consequences on PFM measurements. Note that a little shift of the frequency of the alternating voltage applied to the tip can result in drastic changes of the background signal which in turn are followed by significant changes in the PFM images obtained with the  $P_R$  signal. Several surprising features concerning the domain contrast as well as the shape and location of domain boundaries turn out to possibly originate from the system-inherent background. Of course, also physical effects can influence the domain contrast or the domain boundaries, however, a careful analysis of the measured data is mandatory to avoid misinterpretation. In the following, we exemplify the consequences of the background considering some surprising features of PFM imaging:

- Enhancement of the domain contrast
- Nulling of the domain contrast
- Inversion of the domain contrast
- Shift of the domain boundary
- Change of the shape of the domain boundary

The domain contrast  $D$ , as it is observed in PFM measurements when using the magnitude output  $R$  from the lock-in amplifier for image acquisition, is given by  $D = (P_R^{+z} - P_R^{-z})$ . From Fig. 1(a) it is obvious that  $D$  reaches a maximum when  $\phi = 0^\circ$  and  $P_X^b \geq d$ .

A minimum of  $D$ , so called "nulling" of the domain contrast, is observed when  $\phi = 90^\circ$ . In this case  $P_R^{+z} = P_R^{-z}$  and therefore  $D = 0$ , the PFM images show only dark lines at the domain boundaries, where the mechanical deformation is suppressed by clamping because of the different orientation of the domains.

An inversion of the domain contrast can be observed when the  $P_X^b$  changes its sign. This is the case for example when  $\vec{P}^b$  switches from quadrant one  $\rightarrow$  two, therefore  $[P_R^{+z} > P_R^{-z}]$  is replaced by  $[P_R^{+z} < P_R^{-z}]$  and then  $D$  changes its sign. Thus an unambiguous identification of  $\pm z$  domains becomes impossible.

Simple considerations based on the vector diagram of Fig. 1(a) allow to understand the influence of the background signal on the domain contrast. The consequences of the background signal on the location and shape of the domain boundaries in PFM measurements when using the magnitude output from the lock-in amplifier, however, need a more careful

analysis. For a better understanding, two cases will be treated separately: (i)  $\vec{P}^b = P_X^b$  and (ii)  $\vec{P}^b = P_Y^b$ . From Fig. 1(b) it is evident, however, that usually a mixed background  $P_R^b = \sqrt{(P_X^b)^2 + (P_Y^b)^2}$  is present.

For modeling, we approximate the PFM-signal  $P_X$  across a domain boundary with a hyperbolic tangent, i.e.,  $P_X = \tanh s$  with  $s$  denoting the lateral position at the sample surface perpendicular to the domain wall being located at  $s = 0$ , thus the amplitude of the piezoresponse signal  $d$  is normalized to 1.

The width of the domain boundary, i.e., the slope of the hyperbolic tangent, is determined mainly by the tip radius [19]. It must not to be confused with the real width of the domain wall over which the polarization reverses. Here we use a 25% - 75% criterion to determine the width of the domain boundary for the in-phase PFM-signal  $P_X$  which corresponds to the full width half maximum of  $P_R$  PFM-signal.

*Background signal  $\vec{P}^b = P_X^b$*

Adding the background  $P_X^b$  to the PFM-signal leads to:

$$\begin{aligned} P_X &= \tanh s + P_X^b & \Rightarrow & \quad P_R = |\tanh s + P_X^b|, \\ P_Y &= 0 \end{aligned}$$

because  $P_R = \sqrt{(P_X)^2 + (P_Y)^2}$ . The consequences of this simple consideration can be seen in Fig. 2(a) where scan lines across a domain boundary of the  $P_R$  and the  $P_X$  signal are simulated. In the case of no background signal ( $P_X^b = 0$ , thick lines) both readout signals show the domain boundary at its real position  $s = 0$ , in the  $P_R$  signal as a minimum and in the  $P_X$  signal as the inflection point of the slope. However, when adding the background signal  $P_X^b$ , the minimum of  $P_R$  is shifted by  $\Delta s$  pretending the domain boundary to be at a different location.

Figures 2(b) and (c) show images of a single domain boundary recorded simultaneously with the  $P_X$  and  $P_R$  PFM-signals. After the first half of the the image, the frequency of the alternating voltage applied to the tip is changed in order to alter the background. Whereas in the  $P_X$  signal the location of the domain boundary is not affected (Fig. 2(c)) the image taken with the  $P_R$  output shows a distinct shift of the domain boundary (Fig. 2(b)). This pretended shift can be easily calculated to be  $\Delta s = \operatorname{arctanh}(-P_X^b)$ . To give an example, the domain boundary is seemingly shifted by 55 nm for a background signal  $P_X^b = \frac{1}{2}P_X = 0.5$

if the width of the domain wall is measured to be 100 nm. Note that the apparent shift of the domain boundary depends on the tip radius as the slope of the  $P_X$  signal is steeper for sharper tips [19]. As a further consequence of this apparent shift of the domain boundary, a broadening and also an asymmetry is pretended. In the extreme case, when the background signal  $P_Y^b$  is larger than the domain signal no minimum can be observed in the  $P_R$  output channel of the lock-in amplifier at the domain boundary.

*Background signal  $\vec{P}^b = P_Y^b$*

Adding the background  $P_Y^b$  to the PFM-signal leads to:

$$\begin{aligned} P_X &= \tanh s & \Rightarrow & \quad P_R = \sqrt{(\tanh s)^2 + (P_Y^b)^2}. \\ P_Y &= P_Y^b \end{aligned}$$

From Fig. 3(a) it is obvious that for a background signal  $P_Y^b$  PFM images recorded with the  $R$  channel of the lock-in amplifier only show the domain boundaries. Their full-width-half-maximum  $W$  can be calculated to be

$$W = 2 \operatorname{arctanh} \left( \frac{1}{2} \sqrt{1 - 2(P_Y^b)^2 + 2\sqrt{(P_Y^b)^2 + (P_Y^b)^4}} \right)$$

Furthermore, the visibility of the domain boundary decreases with increasing  $P_Y^b$  background signal.

Figures 3(b) and (c) show experimental images of a single domain boundary recorded simultaneously with the  $P_X$  and  $P_R$  PFM-signals. After recording half of the the image, the frequency of the alternating voltage applied to the tip is changed in order to alter the background. Whereas in the  $P_X$  signal no changes can be observed (Fig. 3(c)) the image taken with the  $P_R$  output shows a distinct broadening of the domain wall as well as a faded visibility (Fig. 3(b)). To give an example, the width of the domain boundary is seemingly broadened by 37 nm for a background signal  $P_Y^b = \frac{1}{2}P_X = 0.5$  if the width of the domain wall is measured to be 100 nm.

*Background signal  $P_R^b = \sqrt{(P_X^b)^2 + (P_Y^b)^2}$*

As it was already mentioned, usually a mixed background is present in PFM measurements as it can be clearly seen from the frequency spectrum in Fig. 1(b). This, however, leads to a superposition of the effects described above, and can have therefore serious conse-

quences on the pretended domain contrast as well as on the features of the domain boundary when using the  $R$  output of the lock-in amplifier.

### Background-free PFM imaging

Now the crucial point is: how does one can get reliable data in PFM imaging despite the background signal? Firstly one should be aware that getting rid of the background seems difficult. Its origin is not known yet. Therefore it is not clear how to suppress it. However, fortunately, there is no need for suppressing the background for recording reliable experimental data in PFM imaging because straight information can be obtained when using the  $P_X$  output channel of the lock-in amplifier.

From the experimental side, there is a additional problem arising: Theoretically, the vibration of the surface due to the converse piezoelectric effect should be in-phase with the alternating voltage applied to the tip (at least for frequencies  $< 100$  kHz). Therefore the piezoresponse signal  $\vec{d}$  should only show up in the  $P_X$  channel of the lock-in amplifier. There is, however, always also a small contribution to it in the  $P_Y$  channel, probably because of an electronically governed phase shift of the SFM. In the vector diagram of Fig. 1(a) the piezoresponse signal  $\vec{d}$  would show up slightly tilted. To extract nevertheless correct data from PFM measurements the easiest solution is to set the phase of the lock-in amplifier such that no domain contrast is visible in the  $P_Y$  output channel (thus again  $\vec{d}$  is parallel to the  $P_X$  axis). This corresponds to a rotation of the coordinate system in the vector diagram of Fig. 1(a). An equivalent (and even more precise) solution is a rotation of the coordinate system after image acquisition such that the standard deviation of the out of phase image is minimized.

### Conclusions

In conclusion we have analyzed the influence of the system inherent background on the images of ferroelectric domains obtained with piezoresponse force microscopy concerning domain contrast and domain boundaries. We have pointed out possible origins for misinterpretation of PFM images when using the magnitude output channel of the lock-in amplifier for readout. Finally, we recommended a detection scheme to get reliable data in PFM

imaging.

### **Acknowledgments**

Financial support of the DFG research unit 557 and of the Deutsche Telekom AG is gratefully acknowledged.

---

- [1] M. M. Fejer, G. A. Magel, D. H. Jundt, and R. L. Byer, IEEE J. Quantum Elect. **28**, 2631 (1992).
- [2] K. T. Gahagan, D. A. Scrymgeour, J. L. Casson, V. Gopalan, and J. M. Robinson, Appl. Opt. **40**, 5638 (2001).
- [3] N. G. R. Broderick, G. W. Ross, H. L. Offerhaus, D. J. Richardson, and D. C. Hanna, Phys. Rev. Lett. **84**, 4345 (2000).
- [4] Y. Cho, K. Fujimoto, Y. Hiranaga, Y. Wagatsuma, A. Onoe, K. Terabe, and K. Kitamura, Appl. Phys. Lett. **81**, 4401 (2002).
- [5] E. Soergel, Appl. Phys. B **81**, 729 (2005).
- [6] I. E. Barry, G. W. Ross, P. G. R. Smith and R. W. Eason Appl. Phys. Lett. **74**, 1487 (1999).
- [7] M. Alexe and A. Gruverman, eds., *Nanoscale Characterisation of Ferroelectric Materials* (Springer, Berlin; New York, 2004) 1st ed.
- [8] T. Jungk, A. Hoffmann, and E. Soergel, arXiv.org: cond-mat/0510005 (2005).
- [9] A. Agronin, M. Molotskii, Y. Rosenwaks, E. Strassburg, A. Boag, S. Mutchnik, and G. Rosenman, J. Appl. Phys. **97**, 084312 (2005).
- [10] C. Harnagea, M. Alexe, D. Hesse, and A. Pignolet, Appl. Phys. Lett. **83**, 338 (2003).
- [11] S. Hong, H. Shin, J. Woo, and K. No, Appl. Phys. Lett. **80**, 1453 (2002).
- [12] O. Kolosov, A. Gruverman, J. Hatano, K. Takahashi, and H. Tokumoto, Phys. Rev. Lett. **74**, 4309 (1995).
- [13] M. Labardi, V. Likodimos, and M. Allegrini, Phys. Rev. B **61**, 14390 (2000).
- [14] M. Labardi, V. Likodimos, and M. Allegrini, Appl. Phys. A **72**, S79 (2001).
- [15] D. A. Scrymgeour and V. Gopalan, Phys. Rev. B **72**, 024103 (2005).
- [16] M. Shvabelman, P. Urenski, R. Shikler, G. Rosenman, Y. Rosenwaks, and M. Molotskii, Appl. Phys. Lett. **80**, 1806 (2002).
- [17] C. H. Xu, C. H. Woo, S. Q. Shi, and Y. Wang, Mater. Charact. **52**, 319 (2004).
- [18] M. Jazbinšek and M. Zgonic, Appl. Phys. B **74**, 407 (2002).
- [19] T. Jungk, L. Tian et al. to be published

## Figure captions

Fig. 1 (a) Vector diagram showing the different PFM-signals measured on a  $-z$  and a  $+z$  domain face ( $P_X$  and  $P_Y$ : in-phase and out-of-phase outputs of the lock-in amplifier;  $\vec{P}^{+z}$  ( $\vec{P}^{-z}$ ): PFM-signals measured on a  $+z$  ( $-z$ ) domain face of a ferroelectric sample;  $\vec{P}^b$ : background signal,  $\vec{d}$  ( $-\vec{d}$ ): piezoresponse signal on a  $+z$  ( $-z$ ) domain face). (b) Frequency dependence (10 to 100 kHz) of the background signal  $\vec{P}^b$ , determined on a PPLN surface with a voltage of 10 V<sub>pp</sub> applied to the tip. The circled numbers indicate the four quadrants.

Fig. 2 Influence of the read-out settings of the lock-in amplifier on the detected domain boundary with different background signals. (a) Simple model predictions of the expected PFM-signals where black lines correspond to the  $P_R$  output and gray dashed lines to the  $P_X$  output of the lock in amplifier without ( $P_R^b = 0$ ) and with ( $P_R^b = P_X^b$ ) the presence of a background signal. Measured PFM-images of a domain boundary recorded simultaneously as  $P_R$  (b) and  $P_X$  (c) PFM-signals. During image acquisition, the frequency of the voltage applied to the tip was changed, thereby adding a background signal  $P_X^b$ . Using the  $P_R$  output leads to a pretended shift of the domain boundary (b) whereas the PFM-image recorded with the  $P_X$  output just becomes brighter (c). The line scans are averages over 20 image lines. The image size is  $1 \times 0.5 \mu\text{m}^2$ .

Fig. 3 Influence of the read-out settings of the lock-in amplifier on the detected domain boundary with different background signals. (a) Simple model predictions of the expected PFM-signals where black lines correspond to the  $P_R$  output and gray dashed lines to the  $P_X$  output of the lock in amplifier. Measured PFM-images of a domain boundary recorded simultaneously as  $P_R$  (b) and  $P_X$  (c) PFM-signals. During image acquisition, the frequency of the voltage applied to the tip was changed, thereby adding a background signal  $P_Y^b$ . Using the  $P_R$  output leads to a pretended broadening of the domain boundary (b) whereas the image from the  $P_X$  output is unchanged (c). The line scans are averages over 20 image lines. The image size is  $1 \times 0.5 \mu\text{m}^2$ .

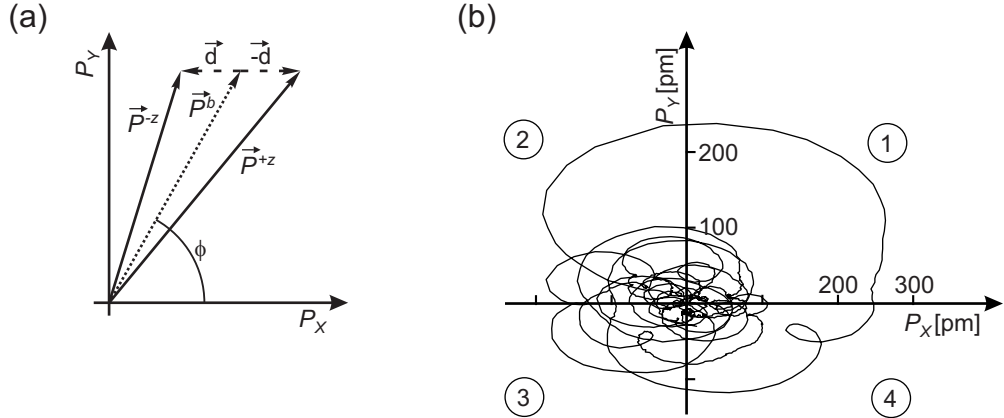


FIG. 1: (a) Vector diagram showing the different PFM-signals measured on a  $-z$  and a  $+z$  domain face ( $P_X$  and  $P_Y$ : in-phase and out-of-phase outputs of the lock-in amplifier;  $\vec{P}^{+z}$  ( $\vec{P}^{-z}$ ): PFM-signals measured on a  $+z$  ( $-z$ ) domain face of a ferroelectric sample;  $\vec{P}^b$ : background signal,  $\vec{d}$  ( $-\vec{d}$ ): piezoresponse signal on a  $+z$  ( $-z$ ) domain face). (b) Frequency dependence (10 to 100 kHz) of the background signal  $\vec{P}^b$ , determined on a PPLN surface with a voltage of 10 V<sub>pp</sub> applied to the tip. The circled numbers indicate the four quadrants.

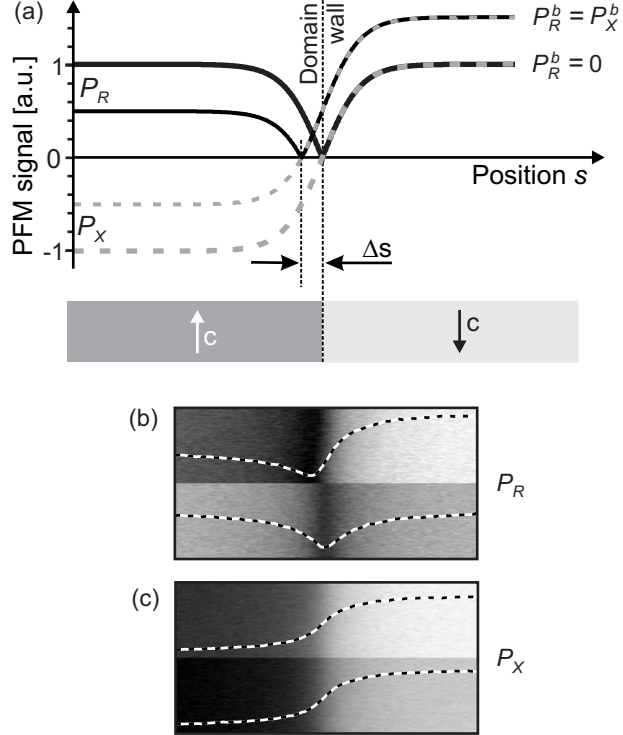


FIG. 2: Influence of the read-out settings of the lock-in amplifier on the detected domain boundary with different background signals. (a) Simple model predictions of the expected PFM-signals where black lines correspond to the  $P_R$  output and gray dashed lines to the  $P_X$  output of the lock in amplifier without ( $P_R^b = 0$ ) and with ( $P_R^b = P_X^b$ ) the presence of a background signal. Measured PFM-images of a domain boundary recorded simultaneously as  $P_R$  (b) and  $P_X$  (c) PFM-signals. During image acquisition, the frequency of the voltage applied to the tip was changed, thereby adding a background signal  $P_X^b$ . Using the  $P_R$  output leads to a pretended shift of the domain boundary (b) whereas the PFM-image recorded with the  $P_X$  output just becomes brighter (c). The line scans are averages over 20 image lines. The image size is  $1 \times 0.5 \mu\text{m}^2$ .

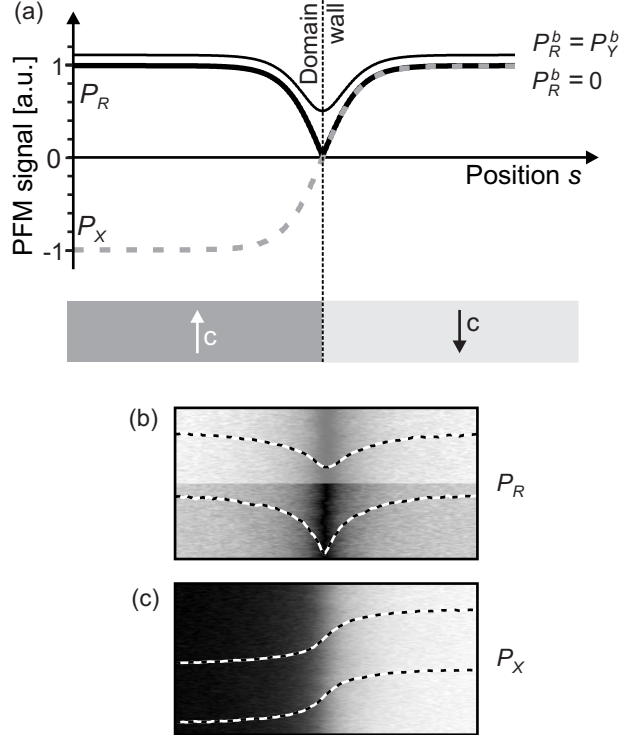


FIG. 3: Influence of the read-out settings of the lock-in amplifier on the detected domain boundary with different background signals. (a) Simple model predictions of the expected PFM-signals where black lines correspond to the  $P_R$  output and gray dashed lines to the  $P_X$  output of the lock in amplifier. Measured PFM-images of a domain boundary recorded simultaneously as  $P_R$  (b) and  $P_X$  (c) PFM-signals. During image acquisition, the frequency of the voltage applied to the tip was changed, thereby adding a background signal  $P_Y^b$ . Using the  $P_R$  output leads to a pretended broadening of the domain boundary (b) whereas the image from the  $P_X$  output is unchanged (c). The line scans are averages over 20 image lines. The image size is  $1 \times 0.5 \mu\text{m}^2$ .